



Oriented External Electric Fields Regulating the Reaction Mechanism of CH₄ Oxidation Catalyzed by Fe(IV)-Oxo-Corrolazine: Insight from Density Functional Calculations

OPEN ACCESS

Edited by:

Miquel Solà,
University of Girona, Spain

Reviewed by:

Sam P. De Visser,
The University of Manchester,
United Kingdom
Miquel Torrent Sucarrat,
University of the Basque Country,
Spain
Thijs Stuyver,
Massachusetts Institute of
Technology, United States

*Correspondence:

Jin-Xia Liang
liangjx2009@163.com
Chun Zhu
czhu2014@163.com

Specialty section:

This article was submitted to
Theoretical and Computational
Chemistry,
a section of the journal
Frontiers in Chemistry

Received: 16 March 2022

Accepted: 08 June 2022

Published: 29 June 2022

Citation:

Wu J, Long T, Wang H, Liang J-X and
Zhu C (2022) Oriented External Electric
Fields Regulating the Reaction
Mechanism of CH₄ Oxidation
Catalyzed by Fe(IV)-Oxo-Corrolazine:
Insight from Density
Functional Calculations.
Front. Chem. 10:896944.
doi: 10.3389/fchem.2022.896944

Jie Wu, Tairen Long, Haiyan Wang, Jin-Xia Liang* and Chun Zhu*

School of Chemistry and Chemical Engineering, Guizhou University, Guiyang, China

Methane is the simplest alkane and can be used as an alternative energy source for oil and coal, but the greenhouse effect caused by its leakage into the air is not negligible, and its conversion into liquid methanol not only facilitates transportation, but also contributes to carbon neutrality. In order to find an efficient method for converting methane to methanol, CH₄ oxidation catalyzed by Fe(IV)-Oxo-corrolazine (Fe(IV)-Oxo-Cz) and its reaction mechanism regulation by oriented external electric fields (OEEFs) are systematically studied by density functional calculations. The calculations show that Fe(IV)-Oxo-Cz can abstract one H atom from CH₄ to form the intermediate with OH group connecting on the corrolazine ring, with the energy barrier of 25.44 kcal mol⁻¹. And then the product methanol is formed through the following rebound reaction. Moreover, the energy barrier can be reduced to 20.72 kcal mol⁻¹ through a two-state reaction pathway. Furthermore, the effect of OEEFs on the reaction is investigated. We found that OEEFs can effectively regulate the reaction by adjusting the stability of the reactant and the transition state through the interaction of electric field-molecular dipole moment. When the electric field is negative, the energy barrier of the reaction decreases with the increase of electric intensity. Moreover, the OEEF aligned along the intrinsic Fe–O reaction axis can effectively regulate the ability of forming the OH on the corrolazine ring by adjusting the charges of O and H atoms. When the electric field intensity is –0.010 a.u., the OH can be directly rebounded to the CH₃· before it is connecting on the corrolazine ring, thus forming the product directly from the transition state without passing through the intermediate with only an energy barrier of 17.34 kcal mol⁻¹, which greatly improves the selectivity of the reaction.

Keywords: density functional calculations, Fe(IV)-Oxo-Corrolazine, CH₄ oxidation, oriented external electric fields, catalysis

1 INTRODUCTION

Compared with oil or coal, methane is an environment-friendly energy, but it is also a greenhouse gas, and its greenhouse effect is much larger than that of carbon dioxide (Chong et al., 2016; Huang et al., 2018; Denning et al., 2021; Huang et al., 2021; Sánchez-López et al., 2021). A quarter of the greenhouse effect caused by man-made greenhouse gases is caused by the leakage of methane into the atmosphere (Kemp et al., 2016). In 2021, the United Nations called for a reduction in methane emission in the atmosphere, aiming to reduce global methane emission by 30% by the end of the century (Brenneis et al., 2022). Therefore, if an efficient method can be found to convert methane into methanol efficiently and economically, it can not only solve the difficulty of methane transportation, but also provide a large number of cheap raw materials for industrial production and reduce methane pipelines leakage (Park et al., 2019; Yan et al., 2020; Januario et al., 2021), thus providing feasible methods for methane emission reduction.

The high valent metal-oxygen systems have been characterized as key intermediates of heme and non heme enzymes (Solomon et al., 2000; Ogliaro et al., 2001; Meunier et al., 2004; Shaik et al., 2005; Rittle and Green, 2010; Visser et al., 2013; Adam et al., 2018; Huang and Groves, 2018; Dubey and Shaik, 2019; Ehdin et al., 2019; Cummins et al., 2020; Shaik and Dubey, 2021), which can effectively hydroxylate aliphatic hydrocarbons (Altun et al., 2007; Hazan et al., 2007), epoxidation (Niwa and Nakada, 2012; Nayak et al., 2020), halogenation (Liu and Groves, 2015), N-demethylation (Yang et al., 2018), and dehydrogenation reactions (Kumar et al., 2009). In particular, Fe(IV)-oxo porphyrin π -cation radical species, known as Cpd-I in heme proteins such as cytochrome P450, can mediate many key oxidative processes (Meunier et al., 2004; Shaik et al., 2005; Cho et al., 2012; Zhang et al., 2017; Caddell Haatveit et al., 2019; Caulfield et al., 2019). Corrolazines, formed by replacing the meso-position carbon atoms of corroles with N atoms, are very similar in structure to porphyrins, but have more π electrons than porphyrins, and can better stabilize high-valent metals (Ramdhanie et al., 2001; Goldberg et al., 2003; Fox et al., 2004; Lansky et al., 2005; Lansky and Goldberg, 2006; Goldberg 2007; McGown et al., 2009; Prokop et al., 2011; Pierloot et al., 2012; Baglia et al., 2015; Joslin et al., 2016; Jung et al., 2016; Zaragoza et al., 2016; Ghosh 2017; Zhu et al., 2018; Dedić et al., 2021; Wang et al., 2021; Zhu et al., 2021). As Fe is the active center metal of methane monooxygenase (Shteinman 2020; Freakley et al., 2021), which can selectively convert methane to methanol under natural environmental conditions. Fe-corrolazine is very likely to catalyze the oxidation of methane to methanol under very mild conditions. Therefore, it is necessary to study the oxidation of methane catalyzed by Fe-Oxo-corrolazine.

Recently, Sason Shaik et al. (Hirao et al., 2008; Gorin et al., 2012; Fried and Boxer, 2015; Li et al., 2015; Akamatsu et al., 2017; Che et al., 2018; Ciampi et al., 2018; He et al., 2018; Yu and Coote, 2019; Shaik et al., 2020; Shaik et al., 2004b; Kraskov et al., 2021; Yu et al., 2021; Zhang et al., 2021; de Visser et al., 2022) found that oriented external electric fields (OEEFs) can be used as a new type of catalyst to catalyze reactions by stabilizing transition states through the interactions between OEEFs and the molecular dipole moments, and even can increase the selectivity of

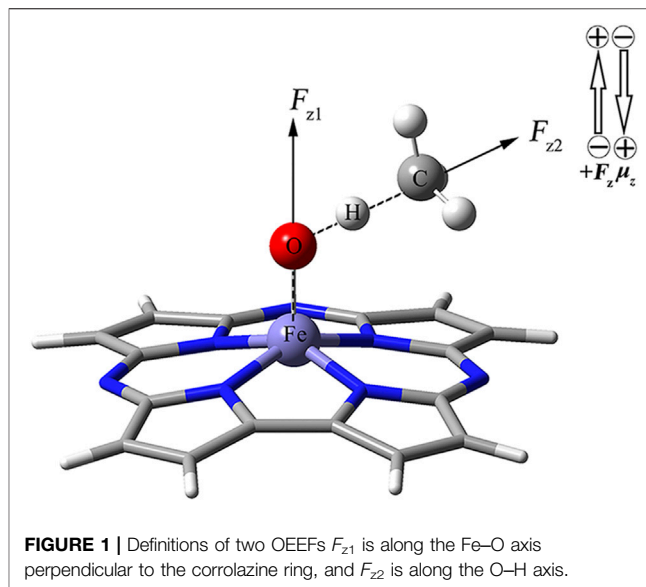


FIGURE 1 | Definitions of two OEEFs F_{z1} is along the Fe–O axis perpendicular to the corrolazine ring, and F_{z2} is along the O–H axis.

reactions through adjusting the direction of OEEFs. Through theoretical calculations, our group also found that the OEEFs can modulate the reaction process through the interactions with the dipole moment of the reaction molecules (Wang et al., 2019).

Herein, we systematically study the reaction process of the oxidation of methane to methanol catalyzed by Fe(IV)-Oxo-corrolazine, and discuss the regulation of its reaction mechanism catalyzed by OEEFs, which provides a theoretical basis for the direct and efficient conversion of methane to methanol.

2 COMPUTATIONAL DETAILS

All the calculations were performed in Gaussian16 package (Frisch et al., 2016), using the B3LYP-D3(BJ) (Stephens et al., 1994; Grimme et al., 2010; Grimme et al., 2011) hybrid functional with the LANL2TZ (Roy et al., 2008) basis set coupled with the effective core potential for Fe atom and the all-electron 6–31++G (d,p) (Hariharan and Pople, 1973) basis set for other atoms. The structures of reactant (RC), transition state (TS), intermediate (INT) and product (P) were fully optimized without any symmetry constraints. Then the natures of these optimized structures were assessed by frequencies calculation, for RC, INT, and P with only real frequencies, and for TS with only one imaginary frequency. Moreover, all TS species were further verified by intrinsic reaction coordinate (IRC) calculations. The calculated output file was analyzed by Multiwfn to obtain the spin density (Lu and Chen, 2012).

As shown in **Figure 1**, using the keyword “Field = $M \pm N$ ”, the two OEEFs, F_{z1} and F_{z2} along the Fe–O axis and O–H axis respectively, were applied to regulate the CH₄ oxidation reaction catalyzed by Fe(IV)-Oxo-Cz. The positive direction of the electric field vector follows the Gaussian 16 convention, i.e., the direction from negative charge to positive charge is $F_z > 0$. The electric field intensity ranges from -0.010 a.u. to $+0.010$ a.u. for F_{z1} and F_{z2} (1 a.u. = 51.4 V \AA^{-1}).

TABLE 1 | Selected Bond Lengths (Å), Mulliken spin density of Fe, and relative energies (ΔG , kcal·mol⁻¹) of Fe(IV)-Oxo-Cz, in doublet, quartet and sextet states.

States	$d_{\text{Fe-N1}}$	$d_{\text{Fe-N2}}$	$d_{\text{Fe-N3}}$	$d_{\text{Fe-N4}}$	$d_{\text{Fe-O}}$	ΔG	spin density
Doublet	1.895	1.895	1.892	1.892	1.568	10.25	0.905
Quarte	1.904	1.904	1.902	1.902	1.615	0	1.259
Sextet	1.910	1.910	1.899	1.899	1.612	40.05	1.253

3 RESULTS AND DISCUSSION

3.1 CH₄ Oxidation Catalyzed by Fe(IV)-Oxo-Corrolazine Under the Field-Free Condition

3.1.1 Structure and Electronic Properties of Fe(IV)-Oxo-Cz

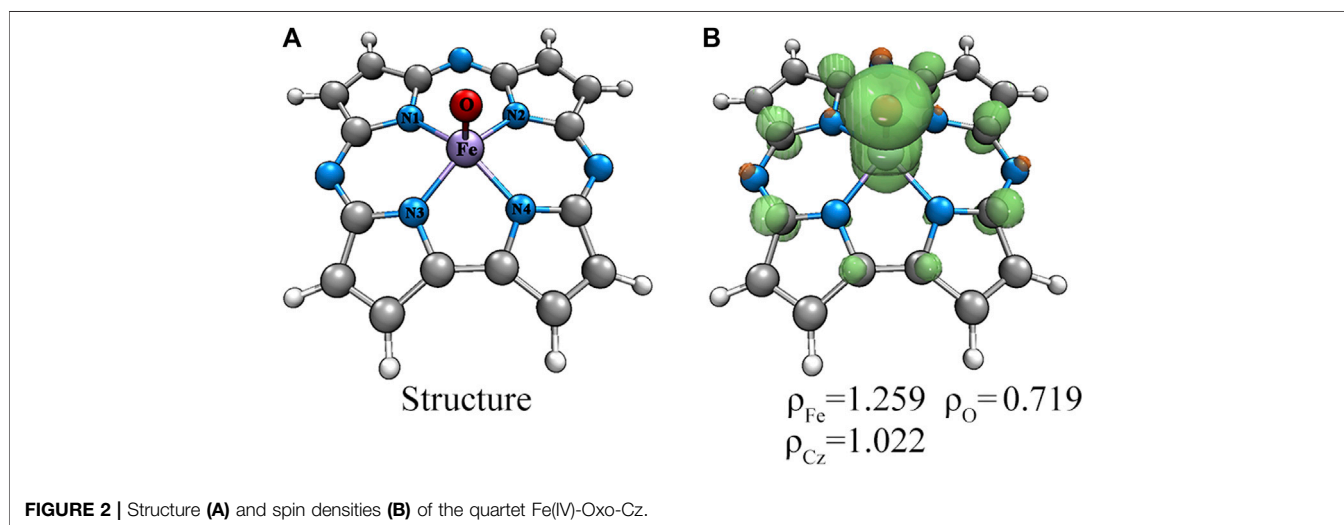
The geometry structures of Fe(IV)-Oxo-Cz in doublet, quartet and sextet states were optimized and their relative energies and selective structure parameters are collected in **Table 1**. As seen from **Table 1**, the quartet state is lower in free energies than the double and sextet states by 10.25 and 40.05 kcal mol⁻¹, respectively (absolute energies in **Supplementary Table S1**). Moreover, the calculated Fe–O bond length in quartet state is 1.615 Å, which is close to the experimentally determined value of 1.640 Å (Cho et al., 2012). Therefore, the quartet state is the ground state, and due to the stronger interaction between the Fe atom and the O atom, the Fe atom deviates upward from the corrolazine ring, as shown in **Figure 2**. Furthermore, the spin densities and NPA charges for the different spin states of Fe(IV)-Oxo-Cz were calculated (see **Supplementary Tables S2, S3**). For the quartet state, the Fe–O moiety only occupied two single electrons, and the remaining one single electron was occupied by the corrolazine ring as shown in **Figure 2**. And the single electron occupying molecular orbitals (SOMO) of the quartet state Fe(IV)-Oxo-Cz is shown in **Figure 3**. Two single electrons are in the orthogonal π orbitals of the Fe–O moiety and the other mainly

distributes on the corrolazine ring, which is exactly the same as the electronic configuration of Cpd-I (Huang and Groves, 2017; Zaragoza et al., 2017), reflecting the potential enzymatic catalytic activity of Fe(IV)-Oxo-Cz.

3.1.2 CH₄ Oxidation Catalyzed by Fe(IV)-Oxo-Corrolazine Under the Field-free Condition

Based on the quartet ground state structure of Fe(IV)-Oxo-Cz, the reaction between Fe(IV)-Oxo-Cz and CH₄ in quartet state in the absence of OEEF was studied. As illustrated in **Figure 4**; **Table 2**, the terminal O of Fe–O first abstracts a hydrogen atom of CH₄, and the bond length of Fe–O bond increases from 1.615 Å of the reactant complex (RC) to 1.725 Å of the transition state (TS1), while the distance between O atom and H atom decreases significantly from 2.393 Å of RC to 1.187 Å of TS1 to yield O–H bond, with the energy barrier of 25.44 kcal mol⁻¹. With the progress of the reaction, the Fe–O bond length grows gradually and the O–H bond length further decreases, yielding the intermediates (INT) of Fe(IV)–OH and CH₃·. Then the product (P) CH₃OH is produced through the rebound reaction where the newly formed OH is rapidly rebounded to the CH₃· from Fe-corrolazine. (Cummins et al., 2020; Huang and Groves, 2017; Shaik et al., 2004a). And in this step, the reaction barrier is only 1.98 kcal mol⁻¹, and the reaction energy of 40.93 kcal mol⁻¹ will promote the reaction to the right.

Moreover, considering that the reaction may proceed at different potential energy surfaces, we further calculated the double state potential energy surface. As shown in **Figure 4** and **Supplementary Table S4**, the TS1 of the double state is lower than that of the quartet state, indicating that the reaction is a two-state reaction and the reaction is easier to carry out (Schröder et al., 2000; Stuyver et al., 2020). However, considering that the quartet state of RC is the ground state, and the quartet state of P is much more stable than the double state, and that when the OEEF with $F_{z1} = -0.010$ a.u. is applied, the energy order of the quartet and double states of reactant dose not changed and there is no energy crossing points along the reaction pathway, so we further



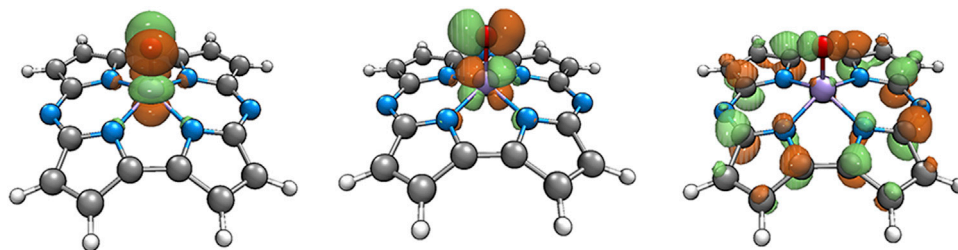


FIGURE 3 | The single electron occupying molecular orbitals of the quartet Fe(IV)-Oxo-Cz.

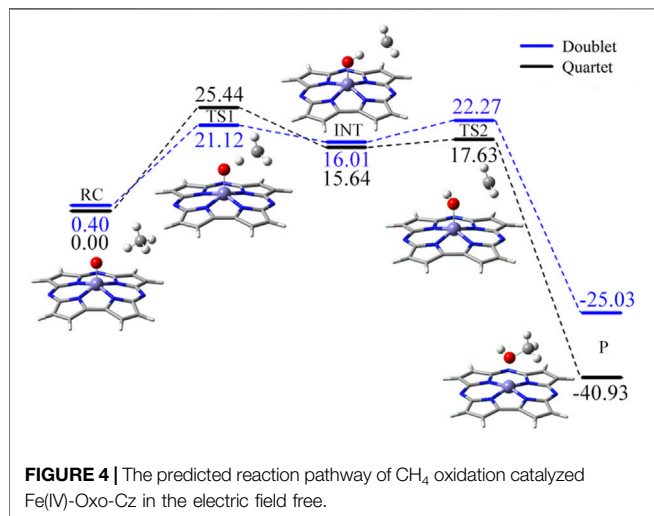


FIGURE 4 | The predicted reaction pathway of CH₄ oxidation catalyzed Fe(IV)-Oxo-Cz in the electric field free.

TABLE 2 | Selected Bond Lengths (Å) and the relative electronic energies (ΔG , kcal·mol⁻¹) of species involved in the reaction of CH₄ oxidation catalyzed for the quartet of Fe(IV)-Oxo-Cz.

Complexes	d _{Fe-O}	d _{O-H}	d _{C-H}	d _{C-O}	ΔG
RC	1.615	2.393	1.092	3.478	0.00
TS1	1.725	1.187	1.353	2.540	25.44
INT	1.780	0.979	2.166	3.142	15.64
TS2	1.811	0.975	2.906	2.880	17.63
P	2.186	0.968	1.998	1.445	-40.93

study the effect of OEEFs on the reaction in quartet state in detail. For comparison, we also selected the representative external electric fields -0.010 , -0.004 , -0.002 , $+0.002$, $+0.004$, and $+0.010$ a.u. for the calculations of the double state reaction, as shown in **Supplementary Tables S5, S6.** As shown in **Supplementary Table S7**, the OEEF does not change the rate-determining step of the reaction.

3.2 OEEFs Regulating the Reaction Mechanism

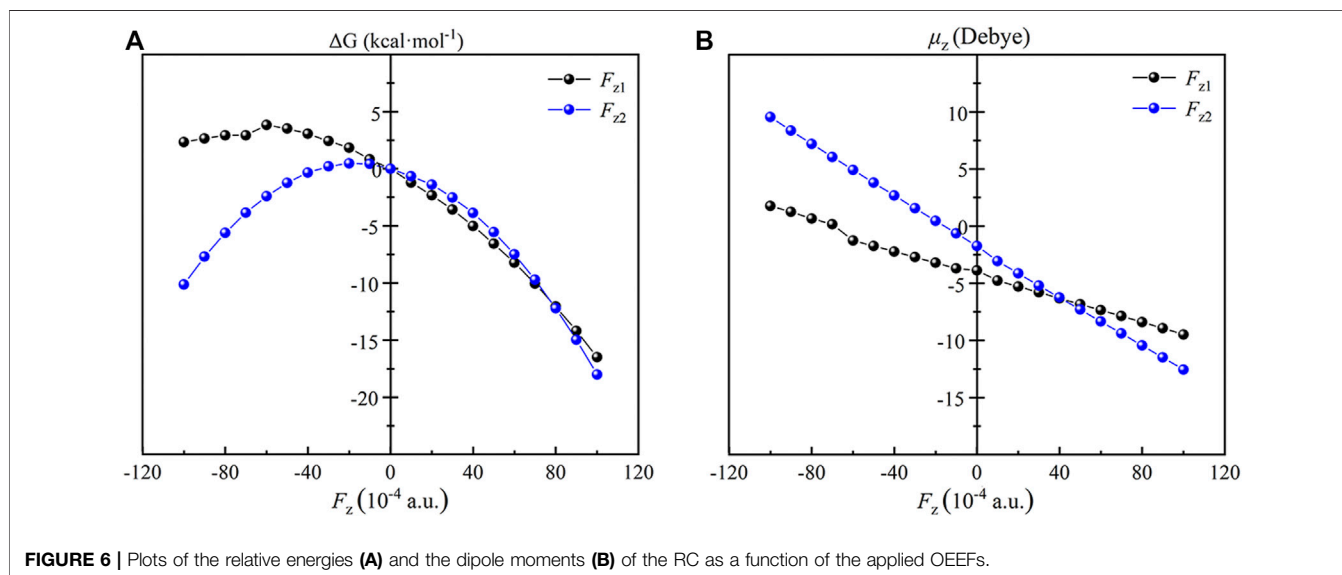
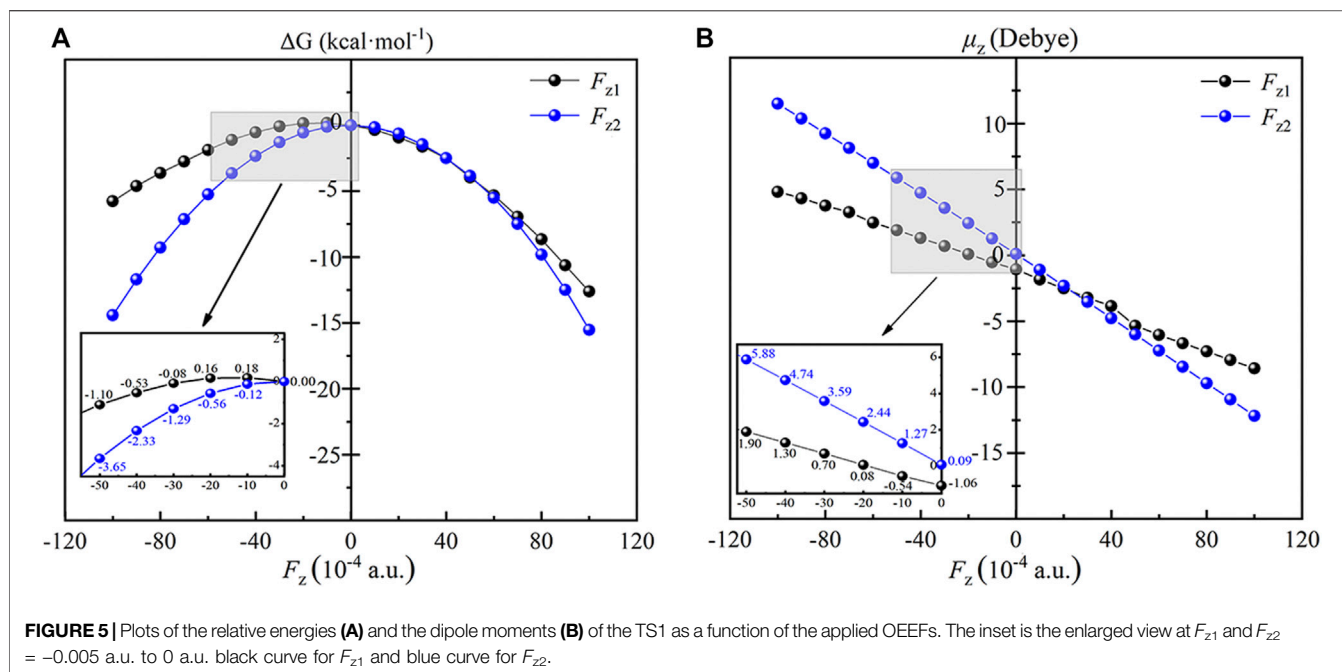
3.2.1 The Effect of OEEF on the Stabilities of the RC and TS1

In order to explore the regulation mechanism of OEEFs in the reaction, we first systematically studied the effect of OEEFs on

the TS1 of the reaction. As shown in **Figure 5A**, due to the application of OEEFs, the relative energies of the reaction TS1 change significantly. For $F_z > 0$, the structure of TS1 is stabilized by OEEFs, and its relative energy decreases with the increase of the electric field intensity. While for $F_z < 0$, OEEFs in different directions have different effects on the TS1. For F_{z1} , when it is in the range of $0 \sim -0.002$ a.u., the TS1 is destabilized by the OEEF, and its relative energy increases with the increase of the electric field intensity. However, as the electric field intensity further increases more than -0.002 a.u. the TS1 is stabilized by the OEEF again, and its relative energy decreases with the increase of the electric field intensity. For F_{z2} , the TS1 is always stabilized by the OEEF, and its relative energy decreases with the increase of the electric field intensity.

To explore the essential reason for the stability change of the TS1 effected by OEEFs, the dipole moments in z orientation of the TS1 of Fe(IV)-Oxo-Cz and CH₄ at different electric field intensities are analyzed. As shown in **Figure 5B**, for $F_{z1} > 0$, the dipole moment in $z1$ direction of the TS1 increases from -1.06 D in the electric field free to -8.58 D in $F_{z1} = +0.010$ a.u. Therefore, the TS1 is stabilized by the applied OEEFs originating from the attractive interaction between the increased dipole moment in $z1$ direction and the OEEF. When the OEEF is reversed to $F_{z1} < 0$, the interaction between the dipole moment and the OEEF becomes complex. For -0.002 a.u. $< F_{z1} < 0$, the OEEF decreases the dipole moment of in $z1$ direction of the TS1, and the repulsion between F_{z1} and the dipole moment of the TS1 destabilizes the TS1. However, when F_{z1} becomes more negative, it flips the orientation of the molecular dipole of the TS1. Therefore, the increasing OEEF increases the dipole moment in $z1$ orientation of the TS1, thus again stabilizing the TS1 originating from the attraction between the increased dipole moment and F_{z1} . For F_{z2} , the orientation of molecular dipole moment in $z2$ direction is opposite to the direction of the OEEF, and the dipole moment always increases with the increase of electric field intensity, thus always stabilizing the TS1 of the reaction originating from the attractive interaction between the increased dipole moment in $z2$ direction and the OEEF.

Similar to the TS1, the RC of the reaction of Fe(IV)-Oxo-Cz and CH₄ are also effected by the OEEF remarkably. As shown in **Figure 6**, for F_{z1} and $F_{z2} > 0$, the dipole moment in z orientation



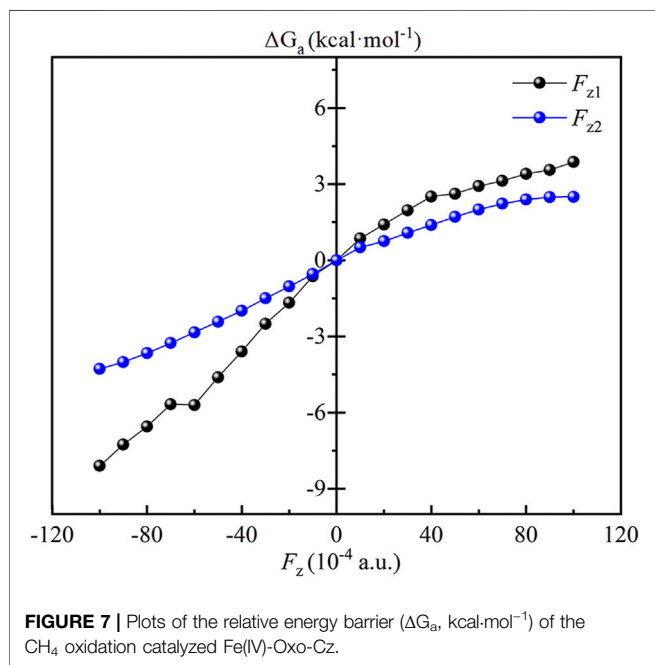
of the RC increases with the increase of OEEFs. Therefore, the RC is stabilized by OEEFs, originating from the attraction between OEEFs and the increased dipole moment in z orientation. For F_{z1} and $F_{z2} < 0$, the dipole moment in z orientation first decreases with the increase of the electric field intensity in the initial part of $F_z < 0$, and then increases with the increase of the electric field intensity, which is more than -0.006 a.u. for F_{z1} and -0.002 a.u. for F_{z2} resulting from the reverse of the molecular dipole in z direction of the RC. Thus, the RC is first destabilized and then stabilized by OEEFs resulting from the repulsion and attraction between OEEFs and the increased dipole moment in z orientation, respectively.

3.2.2 The Effect of OEEFs on the Energy Barrier of CH₄ Oxidation Catalyzed by Fe(IV)-Oxo-Corrolazine

The effect of OEEFs on the energy barrier of the reaction of CH₄ oxidation by Fe(IV)-Oxo-Cz is further investigated. As shown in **Table 3**; **Figure 7**, for F_{z1} and $F_{z2} > 0$, the energy barriers of the reaction increase with the increase of electric field intensity, because the dipole moments in z direction of the RC and TS1 increase with the increase of electric field intensity, and the dipole moments of the RC is always larger than the TS1 in the electric intensity range, thus resulting in its stronger stabilization by OEEFs. However, for F_{z1} and $F_{z2} < 0$, the stabilization of the TS1 by OEEFs is always stronger

TABLE 3 | The dipole moments of the RC, TS1 and the energy barrier (ΔG , kcal·mol⁻¹) of CH₄ oxidation catalyzed by Fe(IV)-Oxo-Cz under different electric field intensities.

F_{z1} (10 ⁻⁴ a.u.)	-100	-80	-60	-40	-20	0	20	40	60	80	100
μ_{z1} (RC)	1.76	0.66	-1.26	-2.23	-3.21	-3.89	-5.28	-6.31	-7.35	-8.40	-9.48
μ_{z1} (TS1)	4.82	3.76	2.48	1.30	0.08	-1.06	-2.52	-3.87	-6.04	-7.29	-8.58
ΔG_{a1}	17.34	18.89	19.74	21.85	23.77	25.44	26.85	27.95	28.36	28.84	29.31
F_{z2} (10 ⁻⁴ a.u.)	-100	-80	-60	-40	-20	0	20	40	60	80	100
μ_{z2} (RC)	9.55	7.20	4.92	2.68	0.46	-1.74	-4.13	-6.24	-8.34	-10.44	-12.56
μ_{z2} (TS1)	11.50	9.26	7.01	4.74	2.44	0.09	-2.32	-4.77	-7.23	-9.70	-12.18
ΔG_{a2}	21.16	21.78	22.60	23.45	24.41	25.44	26.19	26.83	27.44	27.83	27.94



than that of the RC, originating from the stronger dipole moment of the TS1, so the energy barriers of the reaction decrease with the increase of electric field intensity, in which the energy barriers decrease to 17.34 and 21.16 kcal mol⁻¹ for $F_{z1} = -0.010$ and $F_{z2} = -0.010$ a.u., respectively, thus greatly promoting the reaction. Especially for F_{z1} , it can more effectively regulate the reaction than F_{z2} , resulting from its greater slope of energy barrier curve in **Figure 7**. Moreover, as its direction is nearly perpendicular to the corrolazine ring, F_{z1} can be more easily aligned, thus making it easier to apply in practice.

3.2.3 OEEFs Optimizing the Process of CH₄ Oxidation Catalyzed by Fe(IV)-Oxo-Corrolazine

As shown in **Table 4**, for $F_{z1} < 0$, with the increase of electric field intensity, the negative charge of O atom and the positive charge of H atom in the TS1 decrease, while the O–H distance increases. Therefore, the ability of H to transfer to O to form stable the OH groups on the corrolazine ring decreases, which is the key process of forming the INT. When the intensity of the electric field reaches -0.010 a.u., both the negative charge

TABLE 4 | The O–H Lengths (Å), the NPA charges (|e|) of the O and H atoms of the TS1 under different electric field intensities.

F_{z1} (10 ⁻⁴ a.u.)	-100	-80	-60	-40	-20	0
O	-0.402	-0.426	-0.449	-0.471	-0.494	-0.517
H	0.317	0.325	0.334	0.343	0.351	0.361
d_{O-H}	1.309	1.281	1.255	1.232	1.210	1.187
F_{z2} (10 ⁻⁴ a.u.)	-100	-80	-60	-40	-20	0
O	-0.463	-0.474	-0.484	-0.494	-0.505	-0.517
H	0.325	0.331	0.338	0.345	0.353	0.361
d_{O-H}	1.282	1.263	1.245	1.226	1.207	1.187

of the O atom and the positive charge of the H atom reach the smallest, and the OH distance is the largest. Therefore, before the OH group forming on the corrolazine ring, it directly returns to the C atom through the rebound reaction from the P, as shown in **Supplementary Figure S1**, thereby simplifying the process of the reaction without passing through the INT to the product, thus avoiding the coupling between the intermediates to generate other products (Cho et al., 2012), greatly improving the selectivity of the reaction, and being beneficial to industrial applications.

4 CONCLUSION

Extensive density functional calculations have been carried out to explore the CH₄ oxidation reaction catalyzed by Fe(IV)-Oxo-Cz and its regulatory mechanism by OEEFs. The calculations show one H atom of CH₄ is captured by Fe(IV)-Oxo-Cz to form INT, in which OH group is connecting on the corrolazine ring, and then the product methanol is formed through the following rebound reaction. And the energy barrier of the reaction is 25.44 kcal mol⁻¹. Moreover, the energy barrier can be reduced to 20.72 kcal mol⁻¹ through a two-state reaction pathway. To facilitate the reaction, we applied OEEFs F_{z1} and F_{z2} along the Fe–O axis and the O–H axis to modulate the reaction, respectively. When the positive OEEFs are applied, the energy barrier of the reaction increases with the increase of the electric field intensity. However, while flipping OEEFs to the negative direction, the energy barrier of the reaction decreases with the increase of the electric field intensity originating from the interaction of electric field-molecular dipole moment, which

can facilitate the reaction. Especially, the F_{z1} is easier to be applied in practice because its direction is along the intrinsic Fe–O reaction axis approximately perpendicular to the corrolazine ring, and it can effectively modulate the ability of forming the OH on the corrolazine ring by adjusting the charge of O and H atoms. When its intensity is -0.010 a.u., F_{z1} can simplify the reaction path to directly form the reaction product from the transition state without passing through the intermediate, with only an energy barrier of 17.34 kcal mol⁻¹, in which the OH is directly rebounded to CH₃· before it is connecting on the corrolazine ring, thus greatly improving the selectivity of the reaction.

DATA AVAILABILITY STATEMENT

The original contributions presented in the study are included in the article/**Supplementary Material**, further inquiries can be directed to the corresponding authors.

REFERENCES

- Adam, S. M., Wijeratne, G. B., Rogler, P. J., Diaz, D. E., Quist, D. A., Liu, J. J., et al. (2018). Synthetic Fe/Cu Complexes: Toward Understanding Heme-Copper Oxidase Structure and Function. *Chem. Rev.* 118, 10840–11022. doi:10.1021/acs.chemrev.8b00074
- Akamatsu, M., Sakai, N., and Matile, S. (2017). Electric-Field-Assisted Anion-π Catalysis. *J. Am. Chem. Soc.* 139, 6558–6561. doi:10.1021/jacs.7b02421
- Altun, A., Shaik, S., and Thiel, W. (2007). What Is the Active Species of Cytochrome P450 during Camphor Hydroxylation? QM/MM Studies of Different Electronic States of Compound I and of Reduced and Oxidized Iron-Oxo Intermediates. *J. Am. Chem. Soc.* 129, 8978–8987. doi:10.1021/ja066847y
- Baglia, R. A., Prokop-Prigge, K. A., Neu, H. M., Siegler, M. A., and Goldberg, D. P. (2015). Mn(V)(O) versus Cr(V)(O) Porphyrinoid Complexes: Structural Characterization and Implications for Basicity Controlling H-Atom Abstraction. *J. Am. Chem. Soc.* 137, 10874–10877. doi:10.1021/jacs.5b05142
- Brenneis, R. J., Johnson, E. P., Shi, W., and Plata, D. L. (2022). Atmospheric- and Low-Level Methane Abatement via an Earth-Abundant Catalyst. *ACS Environ. Au.* 2, 223–231. doi:10.1021/acsenvironau.1c00034
- Caddell Haatveit, K., Garcia-Borràs, M., and Houk, K. N. (2019). Computational Protocol to Understand P450 Mechanisms and Design of Efficient and Selective Biocatalysts. *Front. Chem.* 6, 663. doi:10.3389/fchem.2018.00663
- Caulfield, K. P., Conradie, J., Arman, H. D., Ghosh, A., and Tonzetich, Z. J. (2019). Iron(II) Corrole Anions. *Inorg. Chem.* 58, 15225–15235. doi:10.1021/acs.inorgchem.9b02209
- Che, F., Gray, J. T., Ha, S., Kruse, N., and ScottMcEwen, S. L. J.-S. (2018). Elucidating the Roles of Electric Fields in Catalysis: A Perspective. *ACS Catal.* 8, 5153–5174. doi:10.1021/acscatal.7b02899
- Cho, K., Leeladee, P., McGown, A. J., DeBeer, S., and Goldberg, D. P. (2012). A High-Valent Iron-Oxo Corrolazine Activates C–H Bonds via Hydrogen-Atom Transfer. *J. Am. Chem. Soc.* 134, 7392–7399. doi:10.1021/ja3018658
- Chong, Z. R., Yang, S. H. B., Babu, P., Linga, P., and Li, X. S. (2016). Review of Natural Gas Hydrates as an Energy Resource: Prospects and Challenges. *Appl. Energy* 162, 1633–1652. doi:10.1016/j.apenergy.2014.12.061
- Ciampi, S., Darwish, N., Aitken, H. M., Diez-Perez, I., and Coote, M. L. (2018). Harnessing Electrostatic Catalysis in Single Molecule, Electrochemical and Chemical Systems: a Rapidly Growing Experimental Tool Box. *Chem. Soc. Rev.* 47, 5146–5164. doi:10.1039/c8cs00352a
- Cummins, D. C., Alvarado, J. G., Zaragoza, J. P. T., Effendy Mubarak, M. Q., Lin, Y.-T., de Visser, S. P., et al. (2020). Hydroxyl Transfer to Carbon Radicals by Mn(OH) vs Fe(OH) Corrole Complexes. *Inorg. Chem.* 59, 16053–16064. doi:10.1021/acs.inorgchem.0c02640
- de Visser, S. P., Mukherjee, G., Ali, H. S., and Sastri, C. V. (2022). Local Charge Distributions, Electric Dipole Moments, and Local Electric Fields Influence Reactivity Patterns and Guide Regioselectivities in α-Ketoglutarate-Dependent Non-heme Iron Dioxygenases. *Acc. Chem. Res.* 55, 65–74. doi:10.1021/acs.accounts.1c00538
- Dedić, D., Dorniak, A., Rinner, U., and Schöfberger, W. (2021). Recent Progress in (Photo-)Electrochemical Conversion of CO₂ with Metal Porphyrinoid Systems. *Front. Chem.* 9, 685619. doi:10.3389/fchem.2021.685619
- Denning, S., Majid, A. A. A., Lucero, J. M., Crawford, J. M., and CarreonKoh, M. A. C. A. (2021). Methane Hydrate Growth Promoted by Microporous Zeolitic Imidazolate Frameworks ZIF-8 and ZIF-67 for Enhanced Methane Storage. *ACS Sustain. Chem. Eng.* 9, 9001–9010. doi:10.1021/acssuschemeng.1c01488
- Dubey, K., and Shaik, S. (2019). Cytochrome P450 -The Wonderful Nanomachine Revealed through Dynamic Simulations of the Catalytic Cycle. *Acc. Chem. Res.* 52, 389–399. doi:10.1021/acs.accounts.8b00467
- Ehudin, M. A., Gee, L. B., Sabuncu, S., Braun, A., Moëne-Locozz, P., Hedman, B., et al. (2019). Tuning the Geometric and Electronic Structure of Synthetic High-Valent Heme Iron(IV)-Oxo Models in the Presence of a Lewis Acid and Various Axial Ligands. *J. Am. Chem. Soc.* 141, 5942–5960. doi:10.1021/jacs.9b00795
- Fox, J. P., Ramdhanie, B., Zareba, A. A., Czernuszewicz, R. S., and Goldberg, D. P. (2004). Copper(III) and Vanadium(IV)-Oxo Corrolazines. *Inorg. Chem.* 43, 6600–6608. doi:10.1021/ic049384a
- Freakley, S. J., Dimitratos, N., Willock, D. J., Taylor, S. H., and KielyHutchings, C. J. G. J. (2021). Methane Oxidation to Methanol in Water. *Acc. Chem. Res.* 54, 2614–2623. doi:10.1021/acs.accounts.1c00129
- Fried, S. D., and Boxer, S. G. (2015). Measuring Electric Fields and Noncovalent Interactions Using the Vibrational Stark Effect. *Acc. Chem. Res.* 48, 998–1006. doi:10.1021/ar500464j
- Frisch, M. J., Trucks, G. W., Schlegel, H. B., Scuseria, G. E., Robb, M. A., Cheeseman, J. R., et al. (2016). *Gaussian 16, Revision A.03*. Wallingford, CT: Gaussian, Inc.
- Ghosh, A. (2017). Electronic Structure of Corrole Derivatives: Insights from Molecular Structures, Spectroscopy, Electrochemistry, and Quantum Chemical Calculations. *Chem. Rev.* 117, 3798–3881. doi:10.1021/acs.chemrev.6b00590
- Goldberg, D. P. (2007). Corrolazines: New Frontiers in High-Valent Metalloporphyrinoid Stability and Reactivity. *Acc. Chem. Res.* 40, 626–634. doi:10.1021/ar700039y
- Goldberg, D. P., Ramdhanie, B., Mandimutsira, B. S., Wang, H., and Fox, J. P. (2003). Corrolazines: Novel Porphyrinoid Compounds Capable of Oxygen

AUTHOR CONTRIBUTIONS

CZ, J-XL, and HW directed the research. JW conducted DFT calculations. JW and TL analyzed the data. All the authors discussed the results and co-write the manuscript.

FUNDING

This work was supported by the National Science Foundation of China (Nos. 21963005, 21763006), Natural Science Foundation of Guizhou University (No. [2021]40 and [2020]32).

SUPPLEMENTARY MATERIAL

The Supplementary Material for this article can be found online at: <https://www.frontiersin.org/articles/10.3389/fchem.2022.896944/full#supplementary-material>

- Binding, Stabilization of High-Valent Metal-Oxo Species, and More. *J. Inorg. Biochem.* 96, 21. doi:10.1016/S0162-0134(03)80440-3
- Gorin, C. F., Beh, E. S., and Kanan, M. W. (2012). An Electric Field-Induced Change in the Selectivity of a Metal Oxide-Catalyzed Epoxide Rearrangement. *J. Am. Chem. Soc.* 134, 186–189. doi:10.1021/ja210365j
- Grimme, S., Antony, J., Ehrlich, S., and Krieg, H. (2010). A Consistent and Accurate Ab Initio Parametrization of Density Functional Dispersion Correction (DFT-D) for the 94 Elements H-Pu. *J. Chem. Phys.* 132, 154104. doi:10.1063/1.3382344
- Grimme, S., Ehrlich, S., and Goerigk, L. (2011). Effect of the Damping Function in Dispersion Corrected Density Functional Theory. *J. Comput. Chem.* 32, 1456–1465. doi:10.1002/jcc.21759
- Hariharan, P. C., and Pople, J. A. (1973). The Influence of Polarization Functions on Molecular Orbital Hydrogenation Energies. *Theor. Chim. Acta (Berl.)* 28, 213–222. doi:10.1007/BF00533485
- Hazan, C., Kumar, D., de Visser, S. P., and Shaik, S. (2007). A Density Functional Study of the Factors that Influence the Regioselectivity of Toluene Hydroxylation by Cytochrome P450 Enzymes. *Eur. J. Inorg. Chem.* 2007, 2966–2974. doi:10.1002/ejic.200700117
- He, Z., Cui, H., Hao, S., Wang, L., and Zhou, J. (2018). Electric-Field Effects on Ionic Hydration: A Molecular Dynamics Study. *J. Phys. Chem. B* 122, 5991–5998. doi:10.1021/acs.jpcc.8b02773
- Hirao, H., Chen, H., Carvajal, M. A., Wang, Y., and Shaik, S. (2008). Effect of External Electric Fields on the C–H Bond Activation Reactivity of Nonheme Iron-Oxo Reagents. *J. Am. Chem. Soc.* 130, 3319–3327. doi:10.1021/ja070903t
- Huang, K., Miller, J. B., Huber, G. W., Dumesic, J. A., and Maravelias, C. T. (2018). A General Framework for the Evaluation of Direct Nonoxidative Methane Conversion Strategies. *Joule* 2, 349–365. doi:10.1016/j.joule.2018.01.001
- Huang, X. Y., and Groves, J. T. (2017). Beyond Ferryl-Mediated Hydroxylation: 40 Years of the Rebound Mechanism and C–H Activation. *J. Biol. Inorg. Chem.* 22, 185–207. doi:10.1007/s00775-016-1414-3
- Huang, X. Y., and Groves, J. T. (2018). Oxygen Activation and Radical Transformations in Heme Proteins and Metalloporphyrins. *Chem. Rev.* 118, 2491–2553. doi:10.1021/acs.chemrev.7b00373
- Huang, Y. F., Shao, Y. M., Bai, Y., Yuan, Q. C., Ming, T. Z., Davies, P., et al. (2021). Feasibility of Solar Updraft Towers as Photocatalytic Reactors for Removal of Atmospheric Methane-The Role of Catalysts and Rate Limiting Steps. *Front. Chem.* 9, 745347. doi:10.3389/fchem.2021.745347
- Januario, E. R., Silvaino, P. F., Machado, A. P., Moreira Vaz, J., and Spinace, E. V. (2021). Methane Conversion under Mild Conditions Using Semiconductors and Metal-Semiconductors as Heterogeneous Photocatalysts: State of the Art and Challenges. *Front. Chem.* 9, 685073. doi:10.3389/fchem.2021.685073
- Joslin, E. E., Zaragoza, J. P. T., Baglia, R. A., Siegler, M. A., and Goldberg, D. P. (2016). The Influence of Peripheral Substituent Modification on P^V, Mn^{III}, and Mn^V(O) Corrolazines: X-Ray Crystallography, Electrochemical and Spectroscopic Properties, and HAT and OAT Reactivities. *Inorg. Chem.* 55, 8646–8660. doi:10.1021/acs.inorgchem.6b01219
- Jung, J., Neu, H. M., Leeladee, P., Siegler, M. A., Ohkubo, K., Goldberg, D. P., et al. (2016). Photocatalytic Oxygenation of Substrates by Dioxxygen with Protonated Manganese(III) Corrolazine. *Inorg. Chem.* 55, 3218–3228. doi:10.1021/acs.inorgchem.5b02019
- Kemp, C. E., Ravikumar, A. P., and Brandt, A. R. (2016). Comparing Natural Gas Leakage Detection Technologies Using an Open-Source “Virtual Gas Field” Simulator. *Environ. Sci. Technol.* 50, 4546–4553. doi:10.1021/acs.est.5b06068
- Kraskov, A., von Sass, J., Nguyen, A. D., Hoang, T. O., Buhrke, D., Katz, S., et al. (2021). Local Electric Field Changes during the Photoconversion of the Bathy Phytochrome Agp2. *Biochemistry* 60, 2967–2977. doi:10.1021/acs.biochem.1c00426
- Kumar, D., Tahsini, L., de Visser, S. P., Kang, H. Y., and KimNam, S. J. W. (2009). Effect of Porphyrin Ligands on the Regioselective Dehydrogenation versus Epoxidation of Olefins by Oxoiron(IV) Mimics of Cytochrome P450. *J. Phys. Chem. A* 113, 11713–11722. doi:10.1021/jp9028694
- Lansky, D. E., and Goldberg, D. (2006). Hydrogen Atom Abstraction by a High-Valent Manganese(V)-Oxo Corrolazine. *Inorg. Chem.* 45, 5119–5125. doi:10.1021/ic060491+
- Lansky, D. E., Mandimutsira, B., Ramdhanie, B., Clausén, M., Penner-Hahn, J., Zvyagin, S. A., et al. (2005). Synthesis, Characterization, and Physicochemical Properties of Manganese(III) and Manganese(V)-Oxo Corrolazines. *Inorg. Chem.* 44, 4485–4498. doi:10.1021/ic0503636
- Li, H. X., Su, T. A., Zhang, V., Steigerwald, M. L., and NuckollsVenkataraman, C. L. (2015). Electric Field Breakdown in Single Molecule Junctions. *J. Am. Chem. Soc.* 137, 5028–5033. doi:10.1021/ja512523r
- Liu, W., and Groves, J. T. (2015). Manganese Catalyzed C–H Halogenation. *Acc. Chem. Res.* 48, 1727–1735. doi:10.1021/acs.accounts.5b00062
- Lu, T., and Chen, F. W. (2012). Multiwfn: A Multifunctional Wavefunction Analyzer. *J. Comput. Chem.* 33, 580–592. doi:10.1002/jcc.22885
- McGown, A. J., Kerber, W. D., Fujii, H., and Goldberg, D. P. (2009). Catalytic Reactivity of a Meso-N-Substituted Corrole and Evidence for a High-Valent Iron-Oxo Species. *J. Am. Chem. Soc.* 131, 8040–8048. doi:10.1021/ja809183z
- Meunier, B., de Visser, S. P., and Shaik, S. (2004). Mechanism of Oxidation Reactions Catalyzed by Cytochrome P450 Enzymes. *Chem. Rev.* 104, 3947–3980. doi:10.1021/cr020443g
- Nayak, M., Nayak, P., Sahu, K., and Kar, S. (2020). Synthesis, Characterization, and Application of Oxo-Molybdenum(V)-Corrolato Complexes in Epoxidation Reactions. *J. Org. Chem.* 85, 11654–11662. doi:10.1021/acs.joc.0c01146
- Niwa, T., and Nakada, M. (2012). A Non-heme Iron(III) Complex with Porphyrin-like Properties that Catalyzes Asymmetric Epoxidation. *J. Am. Chem. Soc.* 134, 13538–13541. doi:10.1021/ja304219s
- Ogliaro, F., Visser, S., Cohen, S., Kaneti, J., and Shaik, S. (2001). The Experimentally Elusive Oxidant of Cytochrome P450: A Theoretical “Trapping” Defining More Closely the “Real” Species. *ChemBiochem* 2, 848–851. doi:10.1002/1439-7633(20011105)2:11<848::AID-CBIC848>3.0.CO;2-0
- Park, M. B., Park, E. D., and Ahn, W.-S. (2019). Recent Progress in Direct Conversion of Methane to Methanol over Copper-Exchanged Zeolites. *Front. Chem.* 7, 514. doi:10.3389/fchem.2019.00514
- Pierloot, K., Langner, E., Swarts, J., Conradie, J., and Ghosh, A. (2012). Low-Energy States of Manganese-Oxo Corrole and Corrolazine: Multiconfiguration Reference Ab Initio Calculations. *Inorg. Chem.* 51, 4002–4006. doi:10.1021/ic201972f
- Prokop, K. A., Neu, H. M., de Visser, S. P., and Goldberg, D. P. (2011). A Manganese(V)-Oxo π -Cation Radical Complex: Influence of One-Electron Oxidation on Oxygen-Atom Transfer. *J. Am. Chem. Soc.* 133, 15874–15877. doi:10.1021/ja2066237
- Ramdhanie, B., Stern, C. L., and Goldberg, D. P. (2001). Synthesis of the First Corrolazine: A New Member of the Porphyrinoid Family. *J. Am. Chem. Soc.* 123, 9447–9448. doi:10.1021/ja011229x
- Rittle, J., and Green, M. T. (2010). Cytochrome P450 Compound I: Capture, Characterization, and C–H Bond Activation Kinetics. *Science* 330, 933–937. doi:10.1126/science.1193478
- Roy, L. E., Hay, P. J., and Martin, R. L. (2008). Revised Basis Sets for the LANL Effective Core Potentials. *J. Chem. Theory Comput.* 4, 1029–1031. doi:10.1021/ct8000409
- Sánchez-López, P., Kotolevich, Y., Yocupicio-Gaxiola, R. I., Antúnez-García, J., Chowdari, R. K., Petranovskii, V., et al. (2021). Recent Advances in Catalysis Based on Transition Metals Supported on Zeolites. *Front. Chem.* 9, 716745. doi:10.3389/fchem.2021.716745
- Schröder, D., Shaik, S., and Schwarz, H. (2000). Two-State Reactivity as a New Concept in Organometallic Chemistry. *Acc. Chem. Res.* 33, 139–145. doi:10.1021/ar990028j
- Shaik, S., Cohen, S., Visser, S., Sharma, P., Kumar, D., Kozuch, S., et al. (2004a). The “Rebound Controversy”: An Overview and Theoretical Modeling of the Rebound Step in C–H Hydroxylation by Cytochrome P450. *Eur. J. Inorg. Chem.* 2004, 207–226. doi:10.1002/ejic.200300448
- Shaik, S., Danovich, D., Joy, J., Wang, Z. F., and Stuyver, T. (2020). Electric-Field Mediated Chemistry: Uncovering and Exploiting the Potential of (Oriented) Electric Fields to Exert Chemical Catalysis and Reaction Control. *J. Am. Chem. Soc.* 142, 12551–12562. doi:10.1021/jacs.0c05128
- Shaik, S., de Visser, S. P., and Kumar, D. (2004b). External Electric Field Will Control the Selectivity of Enzymatic-like Bond Activations. *J. Am. Chem. Soc.* 126, 11746–11749. doi:10.1021/ja047432k
- Shaik, S., and Dubej, K. D. (2021). The Catalytic Cycle of Cytochrome P450: a Fascinating Choreography. *Trends Chem.* 3, 1027–1044. doi:10.1016/j.trechm.2021.09.004
- Shaik, S., Kumar, D., de Visser, S. P., Altun, A., and Thiel, W. (2005). Theoretical Perspective on the Structure and Mechanism of Cytochrome P450 Enzymes. *Chem. Rev.* 105, 2279–2328. doi:10.1021/cr030722j

- Shteinman, A. A. (2020). Bioinspired Oxidation of Methane: From Academic Models of Methane Monooxygenases to Direct Conversion of Methane to Methanol. *Kinet. Catal.* 61, 339–359. doi:10.1134/s0023158420030180
- Solomon, E. I., Brunold, T. C., Davis, M. I., Kemsley, J. N., Lee, S.-K., Lehnert, N., et al. (2000). Geometric and Electronic Structure/Function Correlations in Non-heme Iron Enzymes. *Chem. Rev.* 100, 235–350. doi:10.1021/cr9900275
- Stephens, P. J., Devlin, F. J., Chabalowski, C. F., and Frisch, M. J. (1994). Ab Initio Calculation of Vibrational Absorption and Circular Dichroism Spectra Using Density Functional Force Fields. *J. Phys. Chem.* 98, 11623–11627. doi:10.1021/j100096a001
- Stuyver, T., Ramanan, R., Mallick, D., and Shaik, S. (2020). Oriented (Local) Electric Fields Drive the Millionfold Enhancement of the H-Abstraction Catalysis Observed for Synthetic Metalloenzyme Analogues. *Angew. Chem. Int. Ed.* 59, 7915–7920. doi:10.1002/anie.201916592
- Visser, S., Porro, C., Quesne, M., Sainna, M., and Munro, A. (2013). Overview on Theoretical Studies Discriminating the Two-Oxidant versus Two-State-Reactivity Models for Substrate Monooxygenation by Cytochrome P450 Enzymes. *Curr. Top. Med. Chem.* 13, 2218–2232. doi:10.2174/15680266113136660155
- Wang, C., Danovich, D., Chen, H., and Shaik, S. (2019). Oriented External Electric Fields: Tweezers and Catalysts for Reactivity in Halogen-Bond Complexes. *J. Am. Chem. Soc.* 141, 7122–7136. doi:10.1021/jacs.9b02174
- Wang, X. Q., Wang, H. Y., Zheng, L. F., Zhu, C., and Liang, J.-X. (2021). Oriented External Electric Fields Regulating the Oxidation Reaction of CH₄ Catalyzed by Mn-Corrolazine. *Int. J. Quantum Chem.* 121, e26443. doi:10.1002/qua.26443
- Yan, Y., Chen, C. L., Zou, S. H., Liu, J. J., and XiaoFan, L. P. J. (2020). High H₂O₂ Utilization Promotes Selective Oxidation of Methane to Methanol at Low Temperature. *Front. Chem.* 8, 252. doi:10.3389/fchem.2020.00252
- Yang, L. L., Chen, X., Qu, Z. X., and Gao, J. L. (2018). Combined Multistate and Kohn-Sham Density Functional Theory Studies of the Elusive Mechanism of N-Dealkylation of N,N-Dimethylanilines Mediated by the Biomimetic Nonheme Oxidant Fe^{IV}(O)(N₄Py)(ClO₄)₂. *Front. Chem.* 6, 406. doi:10.3389/fchem.2018.00406
- Yu, L. J., and Coote, M. L. (2019). Electrostatic Switching between S_N1 and S_N2 Pathways. *J. Phys. Chem. A* 123, 582–589. doi:10.1021/acs.jpca.8b11579
- Yu, S., Vermeeren, P., Hamlin, T. A., and Bickelhaupt, F. M. (2021). How Oriented External Electric Fields Modulate Reactivity. *Chem. Eur. J.* 27, 5683–5693. doi:10.1002/chem.202004906
- Zaragoza, J. P. T., Siegler, M. A., and Goldberg, D. P. (2016). Rhenium(v)-oxo Corrolazines: Isolating Redox-Active Ligand Reactivity. *Chem. Commun.* 52, 167–170. doi:10.1039/C5CC07956J
- Zaragoza, J. P. T., Yosca, T. H., Siegler, M. A., Moenne-Loccoz, P., and GreenGoldberg, M. T. D. P. (2017). Direct Observation of Oxygen Rebound with an Iron-Hydroxide Complex. *J. Am. Chem. Soc.* 139, 13640–13643. doi:10.1021/jacs.7b07979
- Zhang, L., Yang, X. H., Li, S., and Zhang, J. M. (2021). Functionalized Silicon Electrodes toward Electrostatic Catalysis. *Front. Chem.* 9, 715647. doi:10.3389/fchem.2021.715647
- Zhang, X. Q., Li, X.-X., Liu, Y. F., and Wang, Y. (2017). Suicide Inhibition of Cytochrome P450 Enzymes by Cyclopropylamines via a Ring-Opening Mechanism: Proton-Coupled Electron Transfer Makes a Difference. *Front. Chem.* 5, 3. doi:10.3389/fchem.2017.00003
- Zhu, C., Liang, J.-X., and Cao, Z. X. (2018). Mn-O-O Electron Spin Flip Mechanism Triggered by the Visible-Light Irradiation for the Generation of an Active Mn(V)-Oxo Complex from O₂: Insight from Density Functional Calculations. *J. Phys. Chem. C* 122, 20781–20786. doi:10.1021/acs.jpcc.8b05531
- Zhu, C., Liang, J.-X., Meng, Y., Lin, J., and Cao, Z. X. (2021). Mn-corrolazine-based 2D-Nanocatalytic Material with Single Mn Atoms for Catalytic Oxidation of Alkane to Alcohol. *Chin. J. Catal.* 42, 1030–1039. doi:10.1016/S1872-2067(20)63707-X

Conflict of Interest: The authors declare that the research was conducted in the absence of any commercial or financial relationships that could be construed as a potential conflict of interest.

Publisher's Note: All claims expressed in this article are solely those of the authors and do not necessarily represent those of their affiliated organizations, or those of the publisher, the editors and the reviewers. Any product that may be evaluated in this article, or claim that may be made by its manufacturer, is not guaranteed or endorsed by the publisher.

Copyright © 2022 Wu, Long, Wang, Liang and Zhu. This is an open-access article distributed under the terms of the Creative Commons Attribution License (CC BY). The use, distribution or reproduction in other forums is permitted, provided the original author(s) and the copyright owner(s) are credited and that the original publication in this journal is cited, in accordance with accepted academic practice. No use, distribution or reproduction is permitted which does not comply with these terms.